UNCLASSIFIED

AD NUMBER

AD405119

NEW LIMITATION CHANGE

TO

Approved for public release, distribution unlimited

FROM

Distribution authorized to U.S. Gov't. agencies and their contractors; Administrative/Operational Use; APR 1963. Other requests shall be referred to Aeronautical Systems Division, Wright-Patterson AFB, OH 45433.

AUTHORITY

AFWAL ltr, 22 Dec 1983

THIS PAGE IS UNCLASSIFIED

UNCLASSIFIED

AD 405 119

DEFENSE DOCUMENTATION CENTER

FOR

SCIENTIFIC AND TECHNICAL INFORMATION

CAMERON STATION, ALEXANDRIA, VIRGINIA

UNCLASSIFIED

NOTICE: When government or other drawings, specifications or other data are used for any purpose other than in connection with a definitely related government procurement operation, the U. S. Government thereby incurs no responsibility, nor any obligation whatsoever; and the fact that the Government may have formulated, furnished, or in any way supplied the said drawings, specifications, or other data is not to be regarded by implication or otherwise as in any manner licensing the holder or any other person or corporation, or conveying any rights or permission to manufacture, use or sell any patented invention that may in any way be related thereto.

ASD-TDR-63-87

405119

CONSTANT OBLIQUE FIELD, ELECTROSTATIC GENERATOR

405 119

TECHNICAL DOCUMENTARY REPORT NO. ASD-TDR-63-87

April 1963

Directorate of Aeromechanics
Aeronautical Systems Division
Air Force Systems Command
Wright-Patterson Air Force Base, Ohio

Project No. 8128, Task No. 812808

(Prepared under Contract No. AF 33(657)-7769 by
Cosmic, Incorporated, Washington, D. C.
Herman Anton, Dominique Gignoux, John J. Shea, authors)

NO OTS

DDC
RECEIVED
MAY 29 1963
TISIA D

NOTICES

When Government drawings, specifications, or other data are used for any purpose other than in connection with a definitely related Government procurement operation, the United States Government thereby incurs no responsibility nor any obligation whatsoever; and the fact that the Government may have formulated, furnished, or in any way supplied the said drawings, specifications, or other data, is not to be regarded by implication or otherwise as in any manner licensing the holder or any other person or corporation, or conveying any rights or permission to manufacture, use, or sell any patented invention that may in any way be related thereto.

ASTIA release to OTS not authorized.

Qualified requesters may obtain copies of this report from the Armed Services Technical Information Agency, (ASTIA), Arlington Hall Station, Arlington 12, Virginia.

Copies of this report should not be returned to the Aeronautical Systems Division unless return is required by security considerations, contractual obligations, or notice on a specific document.

D

28-6981, 100, 1-21-63

FOREWORD

This report was prepared by Cosmic, Inc., Washington, D.C., under Air Force Contract AF 33(657)-7769 and summarizes the findings of a thirteen-month investigation. This contract was initiated under Project No. 8128, "Power Conversion and Transmission Technology", Task No. 812808, "Electrical Power Conversion".

The work was sponsored and administered by the Flight Accessories Laboratory, Directorate of Aeromechanics, Deputy for Technology, Aeronautical Systems Division, Air Force Systems Command. Captain William Dudley was the project engineer.

The authors wish to thank Captain William Dudley for his continued assistance and advice during the performance of this work.

This report covers work done from 15 November 1961 to 15 February 1963.

ABSTRACT

The principle of operation of the constant oblique field, electrostatic generator is described and the increase in power obtained from a generator featuring this field arrangement is predicted from theoretical investigations. A generator has been built and tested in air and in a vacuum environment of 2×10^{-7} to 7×10^{-7} mmHg. The results of the tests in air have met those anticipated. A five-inch diameter rotor has produced a power of 12.5 watts at 15,000 rpm. The vacuum tests have yielded values somewhat greater than those obtained in air, whereas data from previous experimenters show that an increase in power by a factor of 50-100 should be expected.

This technical documentary report has been reviewed and is approved.

GEORGE W. SHERMAN, Chief
Flight Vehicle Power Branch
Flight Accessories Laboratory

TABLE OF CONTENTS

LIST OF ILLUSTRATIONS

1. Introduction

During the years 1959 and 1960 consideration was given at Cosmic, Inc. to transposing for space application the state of the art of electrostatic generators as it appeared in English, French, and German publications. One of the prime considerations was to maximize the power per unit volume of the electrostatic generator. The investigation was limited to those generators utilizing one or a plurality of conducting carriers and a study was made of the various types known. Following the classification described in Ref. 1, a study was made of the field in the gap and on the surface of the rotor members.

The force on the rotor is tangent to the lines of force of the electrostatic field and, therefore, is perpendicular to the surface of the conducting carrier. Fig. 1 shows the line of force on a rotor member of a single-capacitor, two-element machine. One can see that the surface of the rotor contributes to the energy conversion only at the edges of the rotor blade. On most of the surface of the blade, the lines of force are perpendicular to the direction of the motion and the forces exerted on the surface of the rotor do not contribute to energy conversion. Let us examine what this means in terms of the field in the gap. The rotor-stator gap is submitted to an electric field so that it has an energy density equal to $\frac{1}{2}\varepsilon E^2$ at any given point. This potential energy is released only when an edge is adjacent to this particular point. It is therefore desirable to have an electrostatic generator in which most of the rotor surface would be submitted to active surface forces or, to put it in terms of electrical stresses in the gap, to have a generator in which continuous energy conversion occurs at each point of the gap. Such a hypothetical design is shown in Fig. 2 where a rotor is submitted to the influence of two stators in such a manner that

Manuscript released by the authors 28 February 1963 for publication as an ASD Technical Documentary Report.

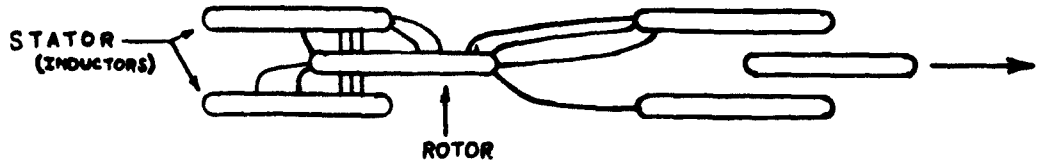

Figure 1. Single Capacitor - Two Element Machine

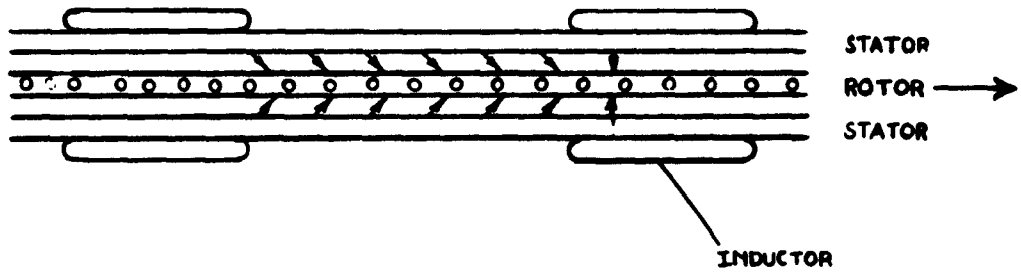

Figure 2. Constant Oblique Field Machine

a constant oblique field is established in the gap. It is to be noted that for a generator in which the size of the stator, rotor and rotor-stator gap are determined, the highest power will be obtained with the constant oblique field generator, assuming that the dielectric medium or vacuum can be submitted to the same electrical stress.

Let us consider the two extreme cases of the oblique field, the cases in which the field is perpendicular or tangential to the rotor surface. In both cases no energy conversion takes place. As will be seen in more detail later, a normal field would correspond to a generator operating under short-circuit conditions so that charges are being carried, thereby creating a normal field without elevation of potential in the longitudinal direction. If the field is tangential to the rotor surface, the rotor carries no charges. However, a difference of potential exists between the input and output poles; this corresponds to the open circuit operation.

It is to be remembered that most generators of the insulating-carrier type feature a constant oblique field. In a Van de Graaff generator the stator consists of a series of rings connected by resistors. This in itself constitutes only a first approximation of a constant oblique field. However, in the generators of the Felici type (Ref. 2) the stator is a continuous flat surface of semi-conducting dielectric, thereby providing a constant oblique field. These generators have reached a fairly high power per unit area of rotor surface. However, this power is not as high as the dielectric properties of the insulating medium (pressurized gases) would permit. This is because the Felici and Van de Graaff generators rely for their operation on ionized zones for commutation, which have a tendency to enhance longitudinal discharges in the gap.

So far, we have only concerned ourselves with a hypothetical field situtation as far as conducting carrier generators are concerned. Fortunately, there exists one type of generator which can be built and which exhibits the remarkable constant oblique field property. The rotor is a combination of insulating and conducting parts. The charge carriers are rods which are not directly adjacent to the gap. They are covered by an insulating material in which they are embedded. The stator consists of a

semi-conducting dielectric. As is the case with most other types of generators, the geometries that can be used would be a belt (not practical here), a cylinder or a disk. The disk appears most practical for space application in that the output can be readily increased by stacking additional disks.

2. Theoretical Investigation

This section summarizes the results of the theoretical studies carried out under this program and contains, i) a discussion of the geometry of the disk type of electrostatic generator considered here, ii) a formulation of a general field-theoretic description of generator performance, iii) a more conventional discussion of the influence of material properties and geometry upon generator output, and iv) a definition of a yardstick useful for comparing generator performance.

2.1 Generator Geometry

The generator considered here consists of three coaxial disks: a central rotor disk and two identical stator disks, disposed symmetrically relative to the rotor and separated from the rotor by an insulating gap of either air at atmospheric pressure or vacuum. The rotor structure is composed of an electrically insulating material, has a thickness 2b and a radius R (Fig. 3) and contains m equally-spaced charge carriers, which are positioned symmetrically relative to the rotor mid-plane. The charge carriers are cylindrical conductors which have a radius a and are disposed radially (i.e., like the spokes of a wheel) between an inner radius λR and an outer radius μR, where $0 < \lambda < \mu \leq 1$. The insulating gap has a thickness d. Each stator disk is composed of a semi-conducting dielectric and has a thickness h. On the outer (relative to the rotor) face of each stator are 2p equally-spaced, radially-tapered inductor electrodes. Each inductor has an angular width Ω and extends radially from λR to μR. To summarize, the geometry of the machine considered here is completely specified by the parameters a, b, d, h, R, λ, μ, Ω and the integers m and p, or equivalently, the angles $\alpha = \pi/p$ and $\beta = 2\pi/m$.

With this generator geometry, it is convenient to introduce a cylindrical coordinate system (s, φ, z) where z is the axial distance along the shaft, s is the radial distance from the shaft and φ is the polar angle. Thus, for example, the rotor volume is defined by

$$\text{Rotor:} \quad -b \leq z \leq +b, \; 0 \leq s \leq R \qquad (1)$$

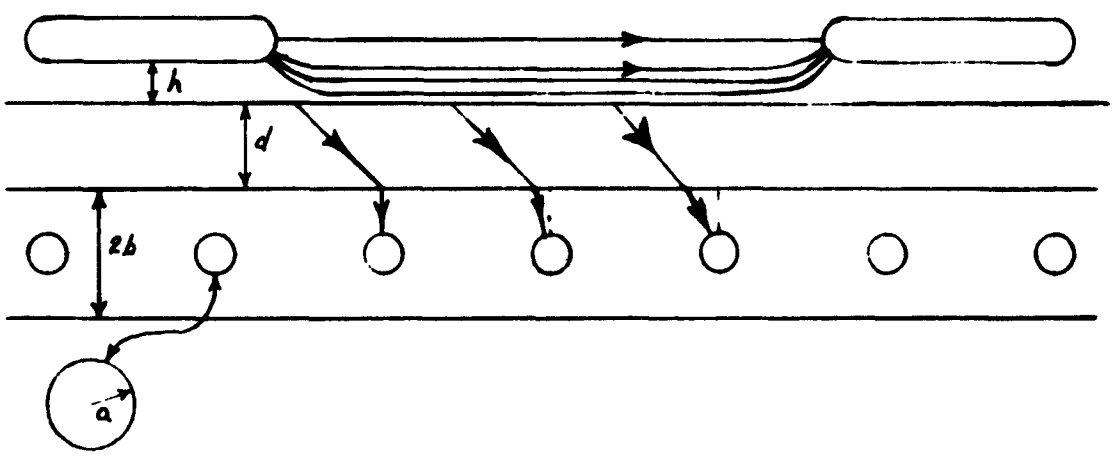

Figure 3. Sketch of Generator Geometry and Field Lines

and the gap and stator volumes are defined analogously. Less trivially, the surface of a charge carrier is defined by

$$s^2 \sin^2(\varphi - \varphi_k) + z^2 = a^2 \qquad \lambda R < s\cos(\varphi - \varphi_k) < \mu R \quad (2)$$

where $\varphi_k = k\beta$

$k = 1, 2, \ldots, m$

2.2 Field-Theoretic Description of Generator Performance

In general, if a force with density $\underline{F}$ acts upon a surface, the elements of which are moving at velocity $\underline{v}$, then the force does work at a rate, W, given by

$$W = \int \underline{F} \cdot \underline{v}\, dS \qquad (3)$$

where the integral is taken over the entire surface in question. (Note that underscored symbols denote vectors). In an electrostatic generator, electric power is obtained by expending mechanical energy to move charged structures through an electric field. In the generator considered here, the only moving charged surfaces are formed by the charge-carriers themselves. The velocity of any point on these surfaces is circumferential with magnitude ωs where $\underline{\omega}$ is the angular velocity of the rotor; the force density at any such point is normal to the surface and has magnitude $\epsilon_r E_c^2/2$, where ϵ_r is the capacitivity of the rotor insulating material and $\underline{E}_c$ is the electric field at the charge-carrier surface. Thus, Equation (3) gives the instantaneous power as

$$W = \int \epsilon_r (E_c^2/2)(\underline{n} \cdot \underline{e}_\varphi)\omega s\, dS \qquad (4)$$

where the integral is taken over all the surfaces, defined by Equation (2), and $\underline{n}$ and $\underline{e}_\varphi$ are the unit vector normal to the charge-carrier surface and the unit vector in the circumferential direction, respectively. It should be noted that those portions of the surface which are moving perpendicular to the local normal contribute nothing.

Equation (4) is rigorously true for an ideal (i.e., loss - less) generator and thus provides the most satisfactory

basis for analyzing generator performance. However, in order to use this approach, it is necessary to predict the field $\underline{E}_c$ at every point on the charge-carrier surfaces. Although this formidable task appears never to have been accomplished for any electrostatic generator, the problem can be formulated as follows. The ingredients of the problem are, in addition to the geometric parameters defined above, the excitation voltage V_{ex} and material properties, such as capacitivity ϵ, dielectric constant κ and volume resistivity ρ or volume conductivity γ. The electrostatic potential ϕ (related to electric field $\underline{E}$ by $\underline{E} = -\nabla\phi$) satisfies Laplace's equation within every homogeneous volume. (For convenience, the potential and other properties in different regions are distinguished by subscripts: c, r, g, s, referring to the charge carriers, rotor, gap, and stator, respectively). The potentials in different regions are patched together by the boundary conditions, which take the following form. The potential of the inductors is specified, while the charge carriers are equipotential surfaces which are cyclically grounded. Since the stator is conducting and the gap is not (except in the air model, when the excitation voltage is above the ionization threshold), true charges appear at the stator-gap interface and the field within the stator is tangential at this surface, as is shown in Fig. 3. At the gap-rotor interface, the normal dielectric refraction takes place and no true charge is present.

Explicit, quantitative statement of the mathematical problem described verbally above has proved extremely valuable for clarifying the roles played by the various ingredients of the problem. However, even under the simplifying and realistic first approximation that radial variations (i.e., dependencies upon s) can be ignored, the problem remains intractable and will not be pursued further here. Rather, we shall turn to more customary and more expedient, albeit less satisfying, means for predicting generator performance.

2.3 Influence of Materials and Geometry Upon Generator Performance

Since several versions of "conventional" theories of electrostatic generator performance are available (Refs. 1, 2, 3, 4, 5), these results are not summarized here, but rather introduced as needed. Generator performance is limited by breakdown

in the gap between rotor and stator. Consequently, to obtain the highest possible field in the gap, the gap thickness is always chosen as small as is consistent with reasonable ease of fabrication. For a given gap thickness and charge-carrier radius, it is instructive to determine the optimal rotor thickness. Since the generator power output is proportional to the charge induced on the charge carrier, we shall take the optimal rotor thickness to be that which results in the largest induced charge on the charge carrier. This charge per unit length, q_c, is given by

$$q_c = C_M V_{ex} \tag{5}$$

where C_M = capacitance, per unit length of charge carrier with respect to inductor at position of maximum capacitance

V_{ex} = excitation voltage

For convenience, we assume that a charge carrier can be treated as a single cylinder embedded in a dielectric slab between plane electrodes. (In other words, we ignore the effects of the other charge carriers). The capacitance C* of the charge carrier, with respect to the rotor face, may be taken as (Ref. 6)

$$C^* = \frac{2\pi\epsilon_r}{\log \frac{4b}{\pi a}} \tag{6}$$

Elementary considerations show that the capacitance C_M, the potential V' of the rotor face, and the field E_g in the gap are given by

$$C_M = \frac{V'}{V_{ex}} C^* \tag{7}$$

$$V' = \frac{b}{\kappa_r d + b} V_{ex} \tag{8}$$

$$E_g = \frac{\kappa_r}{\kappa_r d + b} V_{ex} \tag{9}$$

Substitution of Equations (6) - (9) into (5) gives

$$q_c \approx (2\pi\epsilon_o)\frac{b}{\log \frac{4b}{\pi a}} E_g \qquad (10)$$

For a given gap thickness, the maximum value of E_g is fixed. Consequently, Equation (10) predicts that, for a given gap and charge-carrier size, the induced charge is a minimum for $b/a = e\pi/4 = 2.13$ and increases steadily as b/a is either increased or decreased from that value. Since Equations (6) - (9) are strictly valid only for b large compared to a, conclusions cannot be drawn from (10) regarding values of b/a smaller than 2. However, it appears that the induced charge will be greater for smaller values of b/a, until b/a becomes so small that there is not enough insulating material to smooth the field near the charge carrier. Conversely, increased values of b/a lead to increased values of V_{ex} (V_{ex} increasing linearly with b) and, thus, introduce another limitation on the generator output. In the generators developed under this program, the value of b/a is 4 and was dictated by considerations of mechanical strength and ease of fabrication.

The output power of the generator is proportional to output voltage, which in turn is roughly proportional to the distance between poles (the "constant of proportionality" being an average value of the tangential field, E_φ). Thus, in a sense, increasing the separation between poles may lead to higher outputs; however, for a given-sized generator, increasing the pole separation is equivalent to decreasing the number of poles and thus reducing the power accordingly. An accurate treatment of these conflicting effects must be based upon a detailed field-theoretic study of the variation of tangential field with distance between poles and upon more refined experimental data on the breakdown tangential field as a function of electrode separation.

The semi-conducting dielectric stator serves to smooth out the field and to quench discharges. A lower bound on the resistivity of the stator material can be established by demanding that the backward "quenching" field exceed the sparking field (c.f. Ref. 8). However, a lower bound can also be established by demanding that Joule heating losses in the stator be kept below a prescribed amount. The latter course was followed here, in the equivalent form of demanding that the leakage current not exceed one micro-ampere. For the present geometry and a 20 KV potential

difference between inductors, this is equivalent to requiring that the resistivity exceed 10^8 ohm-meter. The resistivity of the material used here is greater than this by two orders of magnitude. A lower limit on the thickness of the semi-conducting dielectric stator can be set by demanding that the stator not be completely penetrated and punctured by a discharge. Conversely, for a stator thickness which is too large, the lines of force merely tie the inductors together and can reach the stator-gap interface only feebly (Fig. 3). Accurate, quantitative assessment of the influence of the stator geometry and material must be based upon a detailed field-theoretic approach, which includes the effect of the stator dielectric relaxation time in a cyclically varying environment.

One aspect of the influence of the semi-conducting dielectric stator which has been stressed by previous investigators (Ref. 5) is that such a stator serves to limit the variations of the tangential field E_T. Felici (Ref. 5) has pointed out that the variations of E_T induce an additional normal field: however, his demonstrations, while attempting to be general, fail to be convincing for lack of rigor. In the particular case of concern here we shall consider a volume within the gap between rotor and stator defined by

$$b < z < b + d$$

$$\lambda R < s < \mu R$$

and limited by the angles φ and $\varphi + \Delta\varphi$. Let T and N be the components of the electric field in the gap which are circumferential and in the direction of the z-axis, respectively. With these notations Gauss' formula for the volume defined above becomes:

$$2d(\mu - \lambda)RT = \Delta\varphi R^2(\mu^2 - \lambda^2)N \qquad (11)$$

N being the variation of the normal field across the gap.

From (11) we obtain:

$$\Delta N = \frac{d}{R}\frac{dT}{d\varphi} \qquad (12)$$

ΔN may be considered a parasitic normal field generated by the variations of T. Consideration of Fig. 3 shows that it is the thickness of the semi-conducting dielectric which smooths the variation of T.

Decreasing the spacing between charge carriers (or, equivalently, increasing the number of charge carriers) reduces the induced charge per charge carrier and increases the field in the rotor dielectric (by decreasing the effective length of dielectric between input and output brushes). Thus, a limitation on charge-carrier separation is ultimately imposed by the breakdown strength of the dielectric. To discuss the effects of changing charge-carrier separation, it is necessary to consider the mutual influence of charge carriers and, thus, to derive field-theoretically the variation of potential between inductors.

The output power of the machine is the product of output current and voltage. The output current is proportional to the excitation voltage, V_{ex}, while the output voltage is the sum of the excitation voltage and the product of the tangential field E_T, and the distance t, between inductors. Thus, as a function of excitation voltage, the output power W varies as

$$W \sim -V_{ex}(V_{ex} + tE_T) \tag{13}$$

Consequently, W is a maximum for

$$V_{ex} = -\tfrac{1}{2}tE_T \tag{14}$$

2.4 Normalized Power

Since electrostatic machines are built in various configurations and sizes and operate at different speeds, it is useful when comparing performance of such machines to refer to a parameter that expresses the output. Such a parameter is the "normalized power", p, which is defined as the power output divided by the area traversed by the charge carriers and the average linear velocity of the charge carriers and has the units of a pressure which can be expressed in newtons/meter^2 or watts-sec/meter^3. For a cylindrical machine of radius R and length L,

the normalized power is given by

$$p = \frac{W}{(2\pi RL)\omega R} = \frac{W}{2\pi\omega R^2 L} \tag{15}$$

For a disk machine,

$$(\text{Area})(\text{Velocity}) = \int_{\lambda R}^{\mu R} (\omega s)(2\pi s ds) = (2/3)\pi\omega R^3(\mu^3 - \lambda^3)$$

Consequently, for a disk machine with the typical values $\lambda = \frac{1}{2}$, $\mu = 1$ (i.e., the length of the charge carrier is one-half the rotor radius), the normalized power is given by

$$p = \frac{12W}{7\pi\omega R^3} \tag{16}$$

3. Experimental Investigation

3.1 Air-Insulated Model

The air-insulated model of the constant oblique field electrostatic generator was intended to prove the advantages of having a constant oblique field and of having the inductors embedded in a semi-conducting dielectric without having to consider the special requirements necessary to operate in a vacuum environment. To demonstrate best the advantage to be gained by using a semi-conducting dielectric stator two generators were built, one with exposed inductors and one with the inductors embedded in a semi-conducting dielectric.

3.1.1 Design and Fabrication----Air-Insulated Model

The generator could be built with either a cylindrical rotor or a disk rotor. The disk rotor was chosen for this investigation for it was felt that this shape would better lend itself to the many modifications required in the program. The semi-conducting dielectric stator could be fabricated in flat plates rather than in the cylindrical shape which would have been required for a cylindrical machine. The voltage breakdown path along the commutator from one charge carrier to another is greater in a disk machine. The output of the disk machine can be increased by stacking. This will be of future importance.

The rotor has an effective diameter of 5 inches (Figs. 4 and 5). This size was chosen because it was large enough to scale upwards for an optimum machine but small enough to fit in the existing vacuum equipment. The optimum charge-carrier length is one-half the effective rotor radius or 1¼ inches in this case. The charge carriers are 1/16 of an inch in diameter. This size was a good compromise between the small size thought optimum and one that could be machined and handled easily. With the diameter and length of the charge carriers fixed, a spacing of five degrees between charge carriers was chosen, resulting in 72 charge carriers. A 144-charge carrier rotor was also made to determine the effect an increase in the number of charge carriers has on performance. This rotor was fabricated by inserting half-length rods (5/8 inch) between

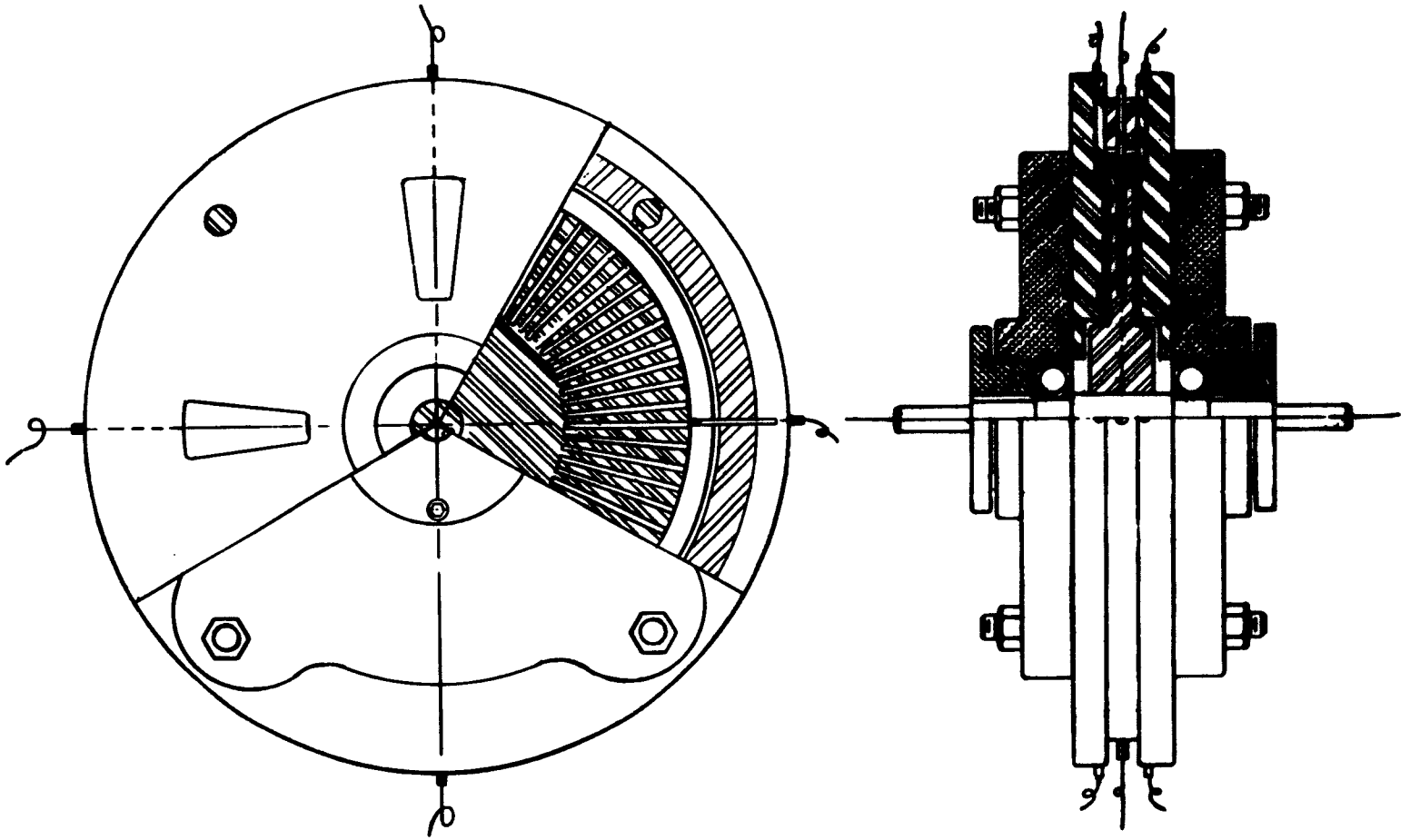

Figure 4. Air-Insulated Constant Oblique Field Electrostatic Generator with Exposed Inductors

Figure 5. Epoxy Rotor with Brush Mounting Ring

the full-length rods (Fig. 6).

The effective diameter and effective radius are measured only to the surface of the commutator. To increase the voltage breakdown distance from the commutator to the inductors, the ends of the charge carriers are located at the bottom of a groove in the rotor. This groove was made one-quarter of an inch deep; therefore, the rotor diameter is actually 5½ inches. The width of the groove is 3/32 of an inch and initially the rotor was ¼ of an inch thick.

The insulating body of the rotor had to have a high volume resistivity and a high dielectric strength, be easily machined, and able to form a good bond with metal. An unfilled epoxy resin, Scotchcast #3, manufactured by Minnesota Mining and Manufacturing Company, was chosen as the insulating material. The volume resistivity of this material is 10^{18} ohm-cm and the dielectric strength is 1,000 to 1,500 volts per mil for a 10-mil thickness. It can be cast readily and is easily machined. The material for the rotor shaft and the charge carriers was chosen to be 303 stainless steel. Precision ball bearings were pressed on the shaft.

The epoxy rotor disk was cast on the shaft, machined to size and then the charge-carrier holes were drilled radially in the disk. The charge carriers were inserted in the holes and bonded in place with epoxy resin. The commutator groove was then machined.

The major and minor diameters of the inductors are the same as those of the charge carriers, 5 inches and 2½ inches, respectively; a four-pole generator was selected. It was thought that the inductors should cover four charge carriers, and therefore, the width of the inductors was fixed at 20 degrees. The material used for the stator plates was Scotchcast #3 epoxy resin, chosen for its high volume resistivity, its dielectric strength, and its machinability. Rather than attach inductors of a conducting material to the stator plates, inductors were formed by machining them in relief in the stator plates and then coating this relief with a silver conducting paint.

The material used for the semi-conducting dielectric

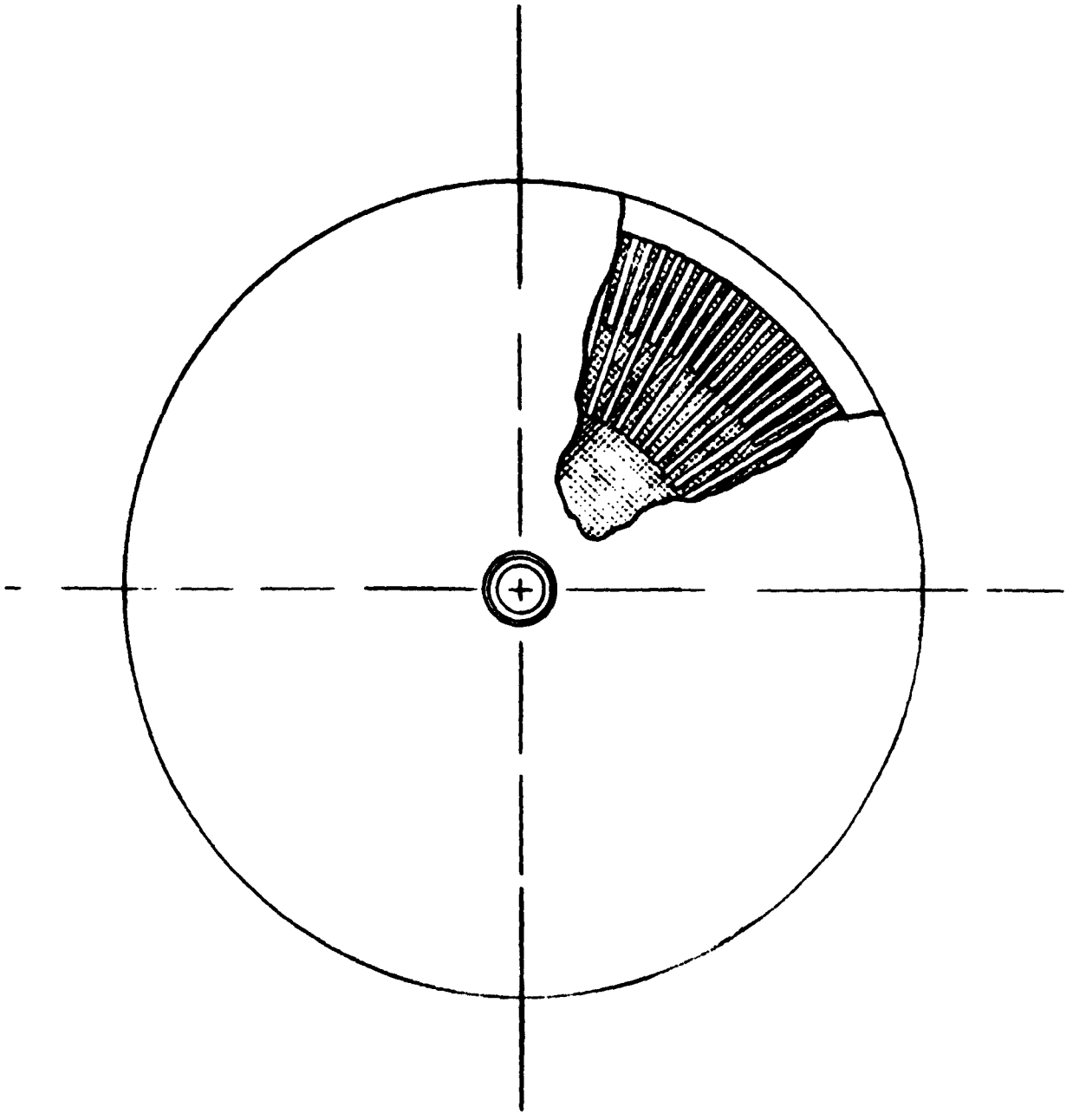

Figure 6. Detail of the 144 Charge Carrier Rotor

stator was soda-lime glass (Corning Type 0080). At 25°C this glass has a volume resistivity of 10^{12} ohm-cm. The inductors were painted on the glass with a silver conducting paint. The plate was covered with silicon grease and pressed against the face of the exposed inductor plate. Contact between the painted inductor and the glass surface was accomplished by use of aluminum foil. This technique allowed maximum use of previously fabricated parts and at the same time permitted ready access to the inductors when modifying the inductors. After concluding the experiment in which the size and shape of the inductors were modified, the glass plates were bonded to insulating glass plates with epoxy resin.

The end plates, which house the bearings and provide a frame for the generator, were machined from 2024 aluminum. Adjustable bearing retainers were provided to permit easy adjustment of the rotor-stator gap.

The first brushes were made from standard carbon brushes and were designed to make contact with the charge carriers. However, it was quickly determined that mechanical contact was not required for commutation--in fact, better results could be obtained without physical contact. One-sixteenth inch, stainless steel rods were substituted for the carbon brushes. These brushes were mounted in a fixture that permitted easy adjustment of the gap and location of the brush. Later, a brush ring was fabricated for multiple brush operation. This ring afforded sensitive adjustment of the brush gap.

3.1.2 Tests----Air-Insulated Model

Tests were conducted to evaluate the performance of the constant oblique field generator with exposed inductors and with inductors embedded in a semi-conducting dielectric. The results demonstrated the advantage to be gained by using a semi-conducting dielectric stator and a constant oblique field. The normalized power was in excess of 20 newtons/meter^2, which approaches that of some vacuum-insulated generators reported to date.

Static tests were conducted on both machines. In the case of the machine with exposed inductors, voltage was applied on all four inductors and the points of highest field concentration

were observed. The contour of the inductors was modified until no points of field concentration could be observed and breakdown occurred from random points on the surface.

Breakdown with the semi-conducting dielectric stator occurred between the ground brush and the excitation lead where it entered the stator. Breakdown did not occur from the inductors.

The rotor was checked for operation up to 15,000 rpm, the limit of the drive. Negligible vibration was encountered.

A corona load was made that could effectively vary the load resistance from zero to the open-circuit resistance of the generator.

During the preliminary tests it was determined, as mentioned in 3.1.1, that brushes making physical contact with the charge carriers were not necessary. It was found that commutation between the brush and the end of the charge carrier occurred before the brush made contact with the charge carrier and that the air adjacent to the brush was constantly ionized. The rods substituted for the carbon brushes were first adjusted with a gap of 0.001 inch. Then this gap was increased. Little difference in output was noticed over a range from 0.001 to 0.010 inch.

The short-circuit output current, as a function of speed with a constant excitation voltage for both stators, was found to be linear--as expected (Fig. 7). Therefore, all tests were conducted with a constant speed drive operating at 3,550 rpm.

The exposed inductor stator was excited and the maximum excitation voltage that could be applied was between 10 and 12 KV. At this voltage, breakdown occurred between the input inductor and the ground brush at the surface of the commutator. The optimum excitation voltage was 6 KV. Increasing the excitation voltage above 6 KV did not increase the output--only the corona on the surface of the inductor.

With the semi-conducting dielectric stator the excitation voltage could be increased to 30 KV before breakdown, which occurred between the ground brush and the excitation lead, where it entered the stator. With the semi-conducting stator the excitation voltage

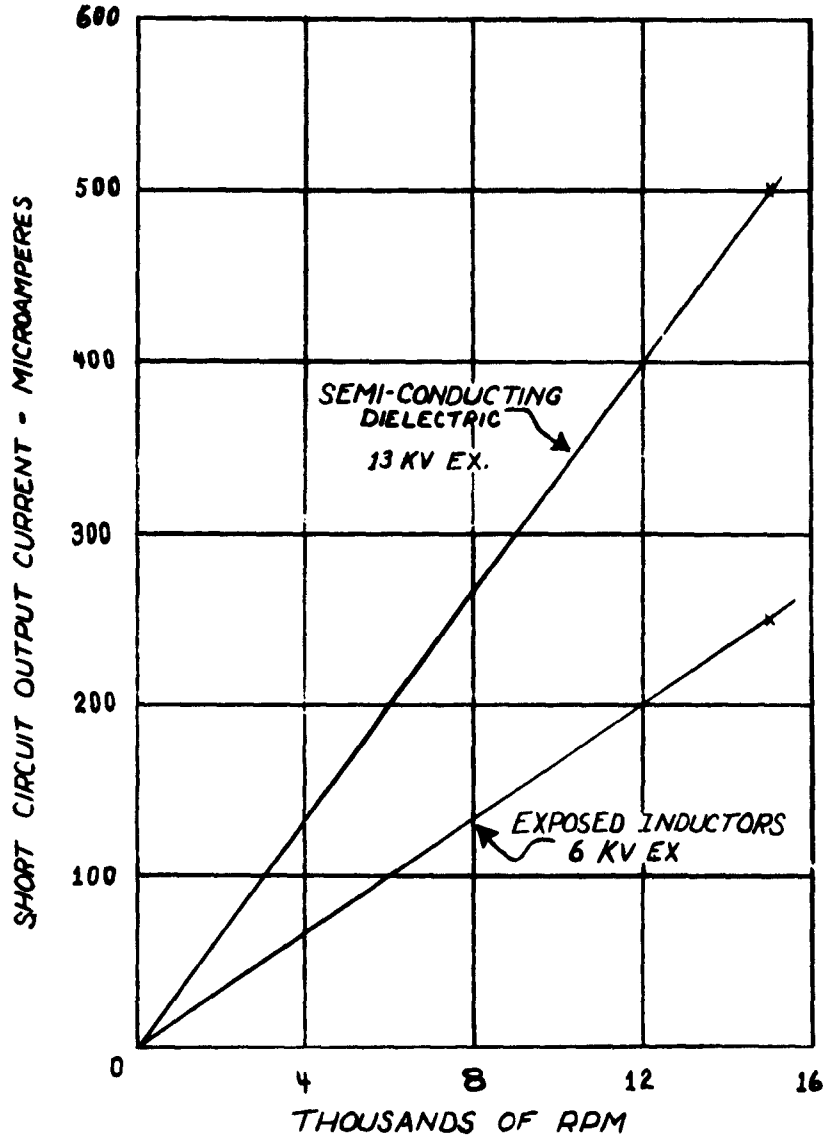

Figure 7. Short Circuit Output Current vs RPM for the Air-Insulated Generator

was not limited by breakdown from the inductor but by the external circuits. Further refinements and shielding of the excitation lead permitted an excitation voltage greater than 30 KV with no flow of excitation current observable. Breakdown was not determined. The value of the excitation voltage at which the output current no longer increased with an increase in excitation voltage was now 15 KV or better than twice that obtained with the exposed inductors.

The short-circuit output current, as a function of excitation voltage, is shown in Fig. 8 for the exposed inductor stator and the semi-conducting dielectric stator. In addition, the output current with an output voltage of 18 KV, as a function of excitation voltage, is shown for the semi-conducting dielectric stator. The dotted lines have been drawn to extend the curves to their point of origin. Commutation does not occur with gap brushes until a minimum excitation voltage; in this case about 3.5 KV is applied. Since the origin is apparently zero, it follows that the brush losses are negligible. The break-off of the curves is due to the ionization of the air in the stator-rotor gap. The short-circuit curve for the exposed inductor stator and for the semi-conducting dielectric stator fall along the same line until ionization occurs. Increasing the dielectric strength of the stator-rotor gap should result in a proportional increase in output.

The output current and output voltage for both stators is shown in Fig. 9. The advantage of the semi-conducting dielectric stator is quite apparent. Not only is a greater output realized with the higher excitation voltage attainable but with the same excitation voltage a higher output voltage can be obtained with a given output current, resulting in a larger power output. With 6 KV excitation the output characteristics for both stators are compared below:

	Iss μa	Voc KV	P_{max} Watts
exposed inductor stator	80	18	0.45
semi-conducting dielectric stator	80	30+	1.0

where Iss is the short-circuit output current and Voc is the open-circuit voltage.

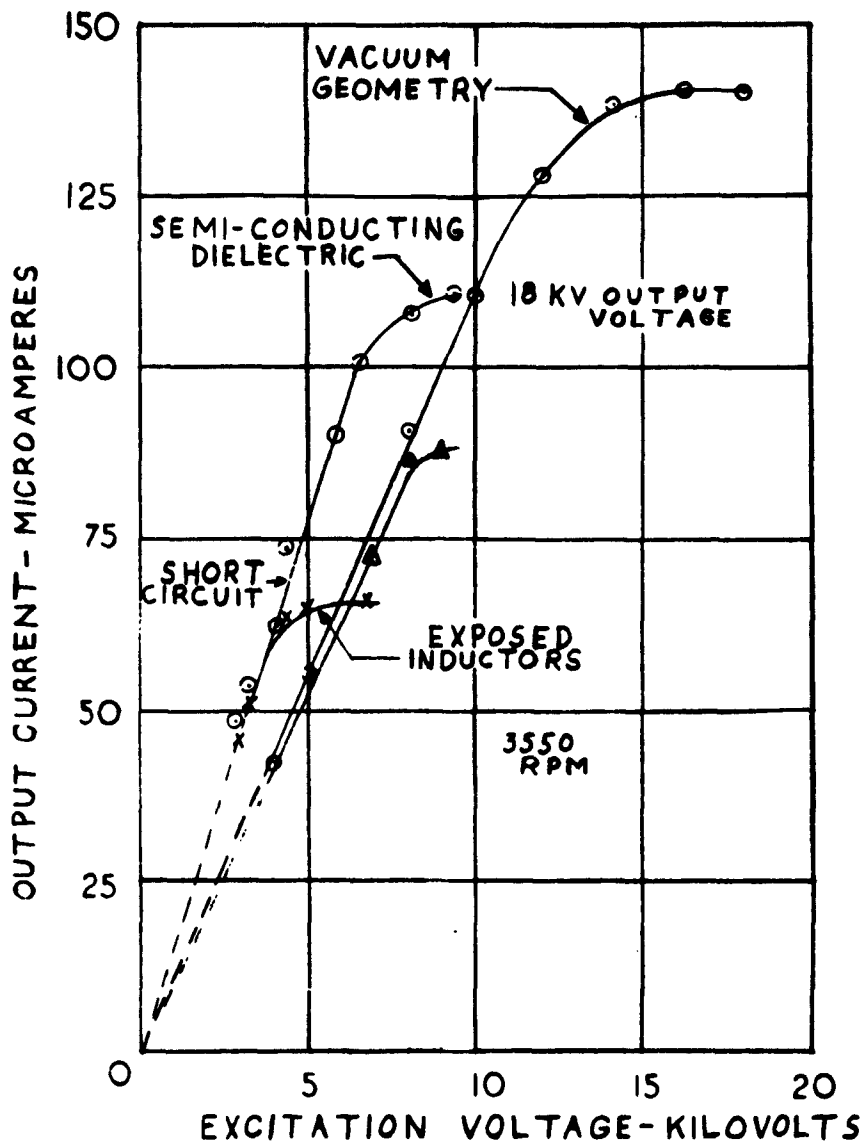

Figure 8. Output Current vs Excitation Voltage for the Air-Insulated Generator

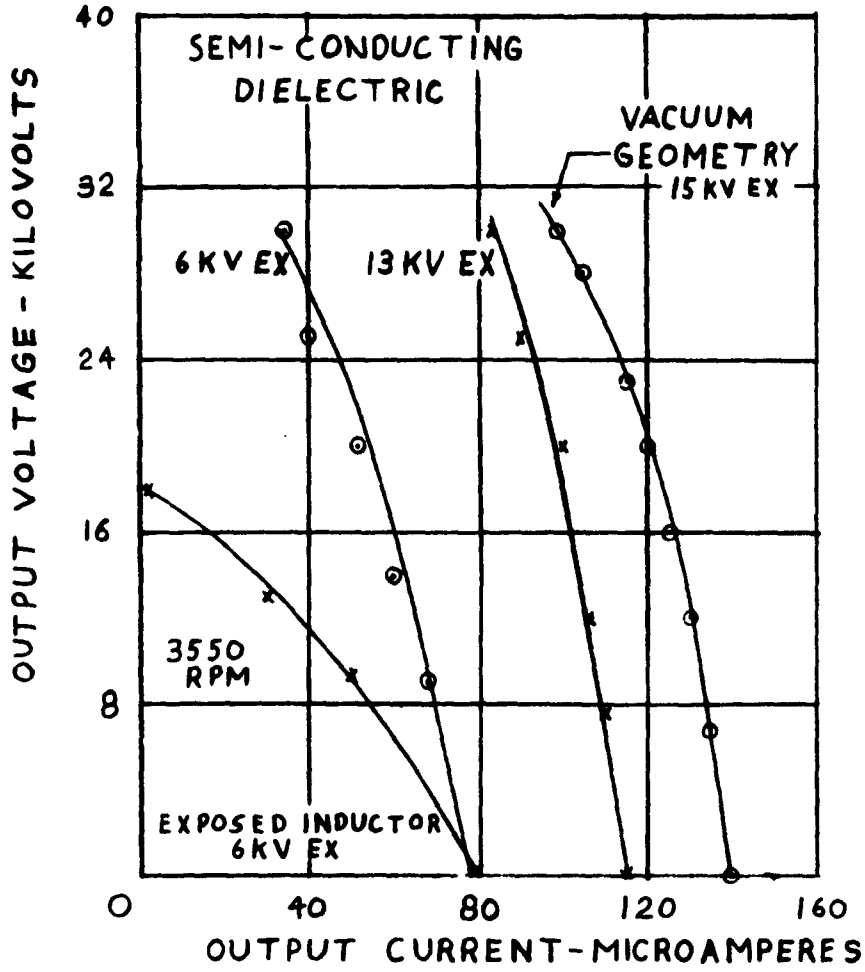

Figure 9. Output Voltage vs Output Current for the Air-Insulated Generator

An additional curve labeled "vacuum geometry" is shown in both Figs. 8 and 9. Both of these curves show the improvement in output obtained using parts from the vacuum generator. Undoubtedly, additional improvements could have been incorporated in the air-model to obtain a slightly greater output but they were deferred to continue with the vacuum tests.

At 3,550 rpm, with 15 KV excitation voltage, the maximum power output is 2.94 watts. The power output realized by using a semi-conducting dielectric stator is better than twice that of the exposed inductor stator with the same excitation voltage and better than five times the power output is realized when the excitation voltage is increased to the maximum effective voltage.

Fig. 10 shows the output current vs. output voltage of the generator for the exposed inductor stator with various width inductors. The inductor with a width of 20° proved to be optimum. The output fell off rapidly with a reduction in width and gradually with an increase in width.

Fig. 11 shows the output current vs. output voltage for the semi-conducting dielectric stator with various width inductors. No difference in output could be noticed for an inductor width of 20° and for a width as narrow as 5°. No tests were made below this width inductor. Since the semi-conducting dielectric is so effective in distributing the excitation potential on the face of the glass plate, the width of the inductors was changed to 5° to make better use of the area of the stator.

An increase in output was obtained with the 144-charge carrier rotor as expected (Fig. 12) but the performance of this rotor was not thoroughly investigated.

The generator is a four-pole machine and can be considered as two machines operating in parallel. One of these machines was connected so as to act as an excitor for the other. Once the circuit was externally primed, the generator operated with no difficulty as a self-excited machine.

The rotor thickness was reduced from 1/4 to 3/16 of an inch and it appeared that the output power increased. However, before this could be established, the rotor was damaged and warped

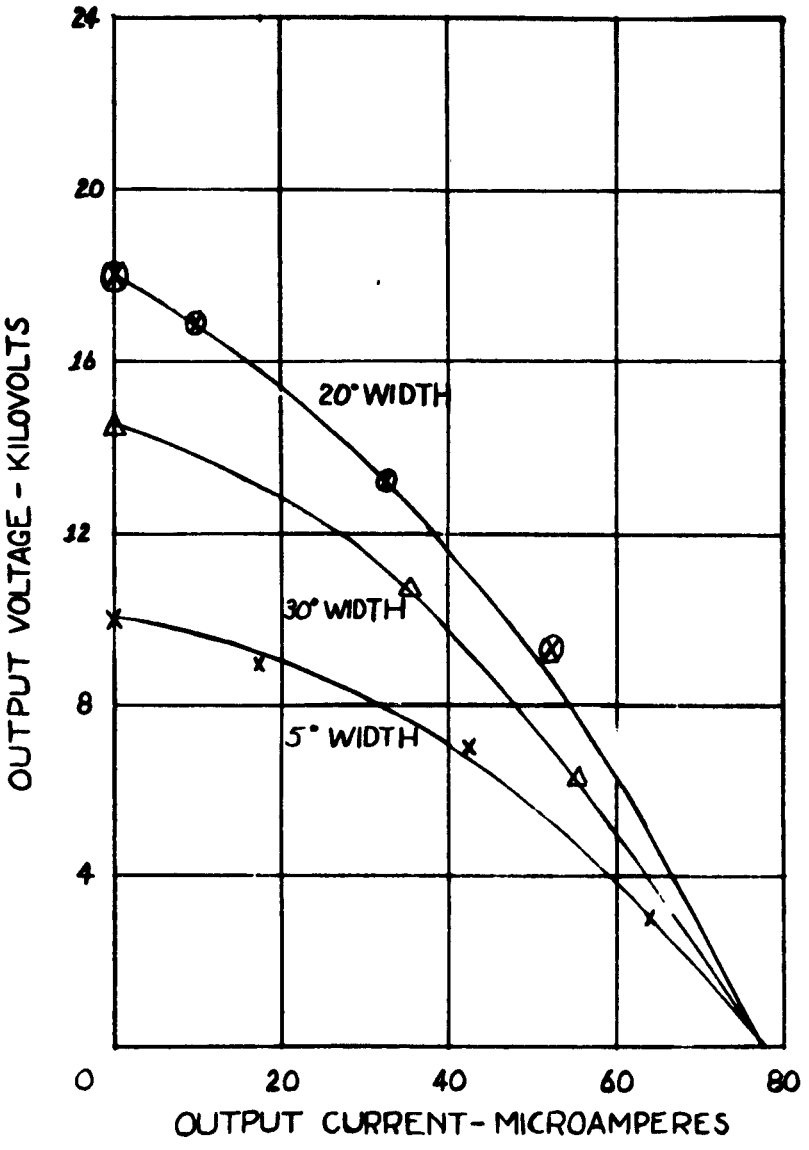

Figure 10. Output Voltage vs Output Current for the Air-Insulated, Exposed Inductor Stator Generator with Various Width Inductors

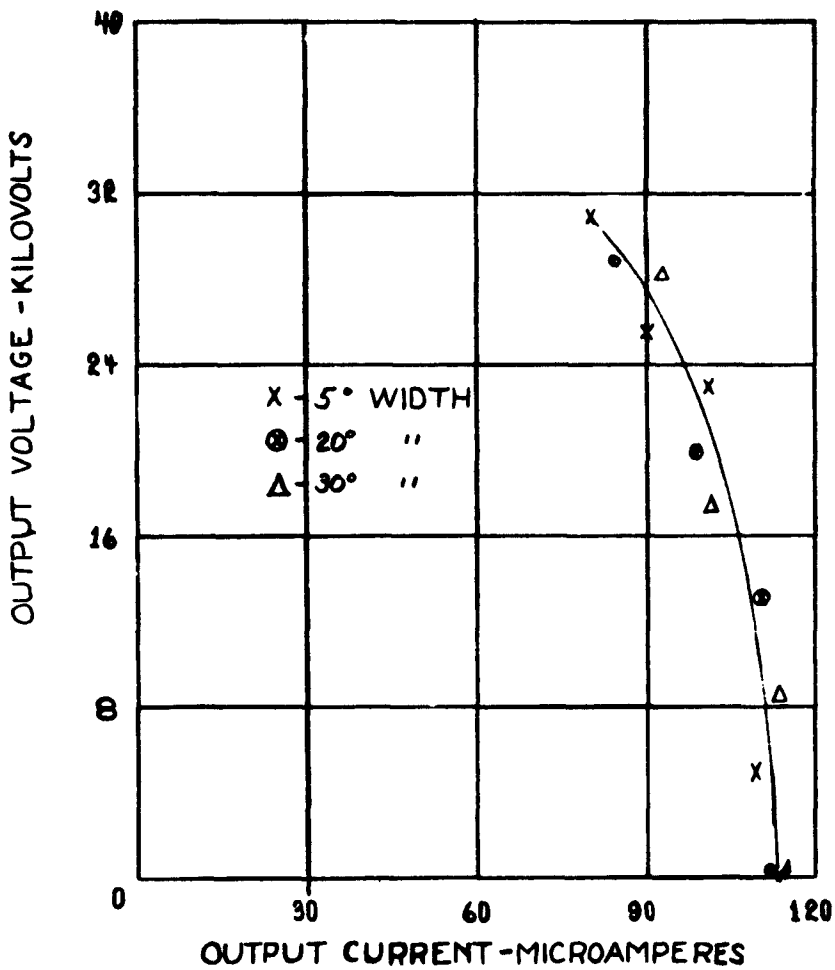

Figure 11. Output Voltage vs Output Current for the Air-Insulated, Semi-Conducting Dielectric Stator Generator with Various Width Inductors

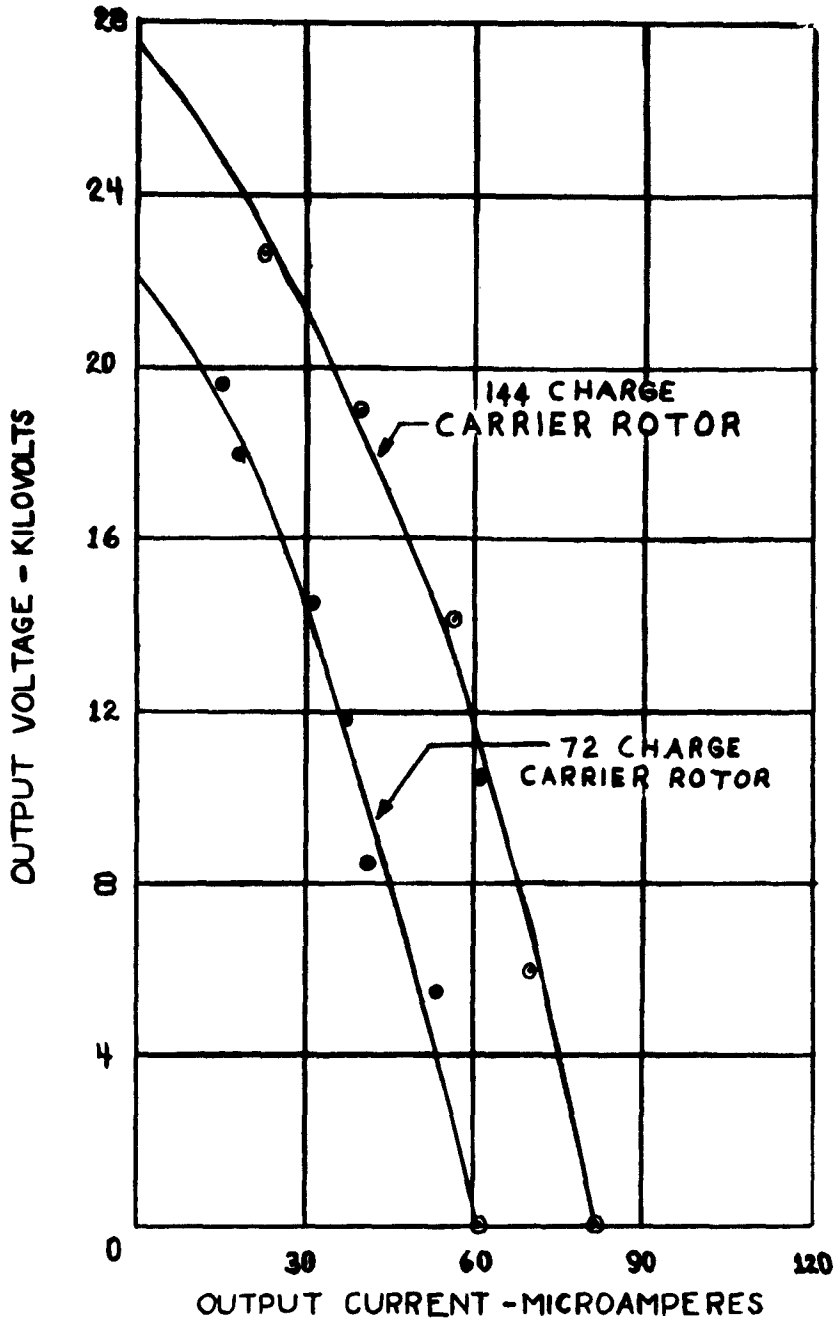

Figure 12. Output Voltage vs Output Current for the Air-Insulated, Semi-Conducting Dielectric Stator Generator Using Only One Stator with Two Different Rotors

enough to require the rotor-stator gap to be increased. With the larger gap, no improvement in output power could be observed.

The air-insulated model has been tested with two stators, one in which the inductors are exposed and one in which the inductors are embedded in a semi-conducting dielectric, over a speed range from zero to 15,000 rpm, with loads that varied from short-circuit to open-circuit and with excitation voltages from zero to values in excess of the optimal excitation voltage. The excitation current is zero up to the point where the optimal excitation voltage is reached in the exposed inductor machine and is zero well past the optimal excitation point in the case of the semi-conducting dielectric machine. The rotor-stator gap breakdown voltage does not affect the generator performance because the optimal excitation point is reached long before breakdown occurs.

Efficiency of the generator is equal to the power output divided by power input. At 3,550 rpm the power output of the semi-conducting dielectric machine is 2.94 watts and the power input from the drive motor is 3.46 watts. Therefore, the efficiency of this machine in air is 2.94/3.46 or 85%. The generator was designed to verify the principle of the oblique field rather than to achieve high efficiency per se. Consequently, little attention was paid to the windage and friction losses and they comprise most of the losses reflected in the efficiency. Now that the principle has been established, the efficiency should be able to be improved significantly.

Fig. 13 shows the partially assembled exposed inductor generator. Fig. 14 shows the partially assembled semi-conducting dielectric generator. Fig. 15 shows the assembled generator with the drive motor in the foreground and the corona load in the background.

3.2 Vacuum Breakdown Investigations

A series of tests have been accomplished to determine to which extent high fields could be obtained between electrodes that are protected by insulating or semi-conducting materials. The most pertinent literature on the subject of vacuum breakdown has been selected from Ref. 7 and has been studied; theoretical

Figure 13. View of the Partially Assembled Air-Insulated Generator with Exposed Inductor Stator in Foreground and 72 Charge Carrier Rotor in Background

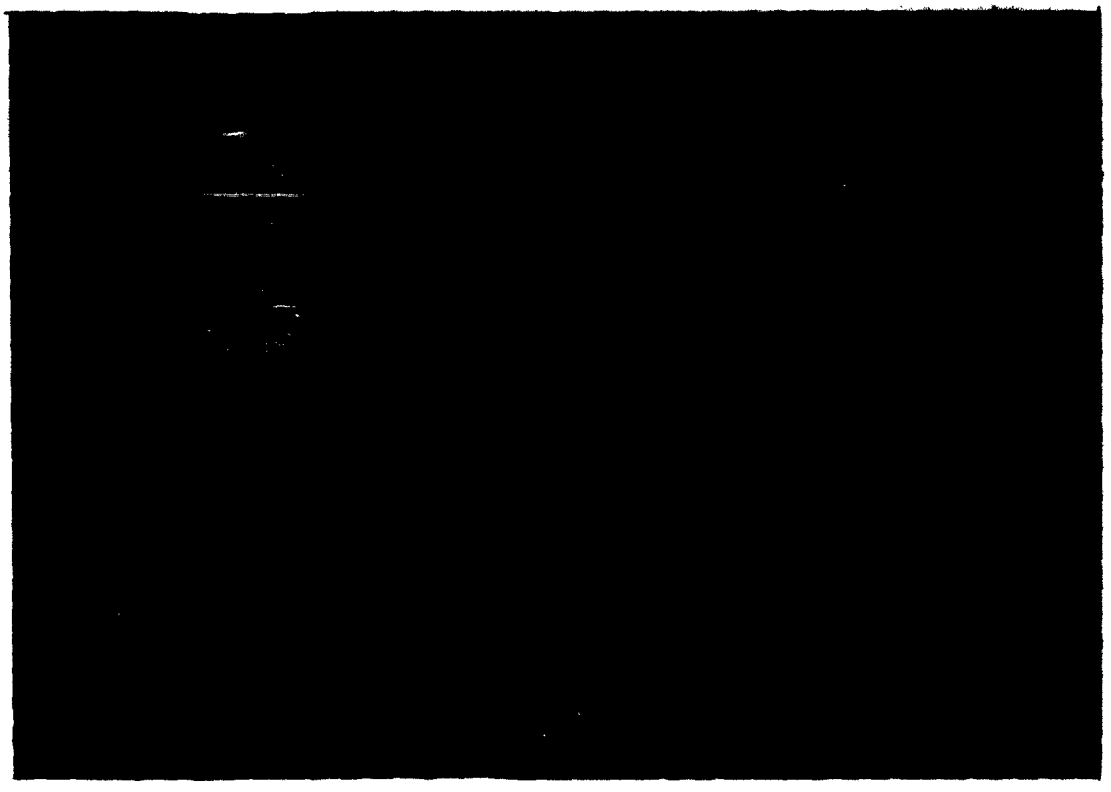

Figure 14. View of the Partially Assembled Air-Insulated Generator with Semi-Conducting Stator

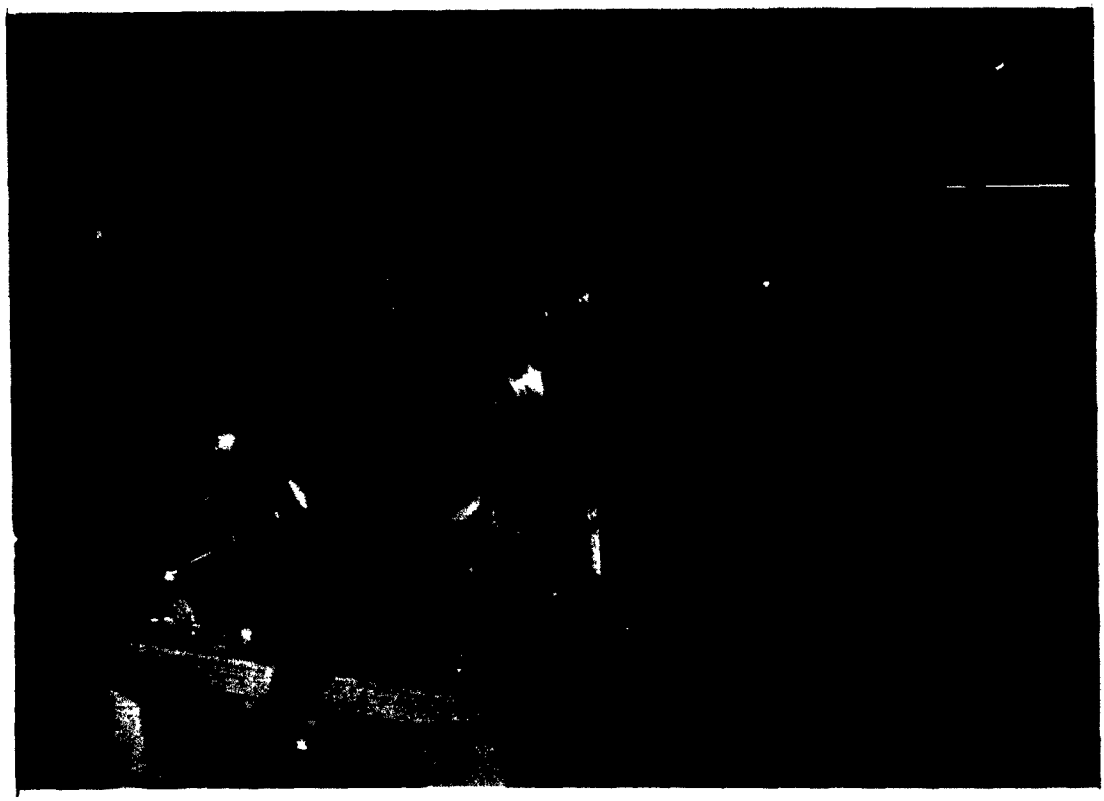

Figure 15. View of the Assembled Air-Insulated Generator with the Drive Motor in the Foreground and the Corona Load in the Background

investigations have predicted that an increase in the field strength could be obtained. These predictions have been confirmed by experiments conducted by Murray (Ref. 8). At the time of writing this report, work accomplished at the Ion Physics Corporation on dielectric coatings (Ref. 9) became available and was examined.

The test setup utilized for the breakdown experiments is that shown in Fig. 16. A polished aluminum sphere is mounted off-center on a vertical shaft. The shaft is mounted on the rotary passthrough by means of a rigid ceramic coupling. The vacuum chamber and its rotary passthrough are described in Section 3.3. Tests were conducted with the sphere being the ground electrode and with the sample consisting of a glass plate with the high voltage electrode being an area covered with baked conducting paint. For a distance of ½ millimeter, breakdown voltage was around 30 kilovolts.

Some questions have been raised as to the applicability to electrostatic generators of the data from tests involving one electrode covered with a dielectric. During static tests the voltage on the surface of the dielectric depends on the relative value of the resistivity of the dielectric as compared to that of the vacuum. The parameter of interest in all electrostatic generators is the field in the gap, whereas the quantity measured in static tests is the voltage between the electrodes; in general, the field in the gap is not equal to the voltage divided by the gap width. To achieve no field or a reduced field in the dielectric requires a time period several orders of magnitude greater than the period of rotation of an electrostatic generator. During one cycle of an electrostatic generator the field varies cyclically and, consequently, there exists a field in the dielectric of the rotor whereas in static tests conducted for a long period of time there may not be a field in the dielectric.

3.3 Vacuum-Insulated Model

The vacuum-insulated model of the constant oblique field electrostatic generator was intended to determine the gain in performance to be realized by operating the machine in a high vacuum environment.

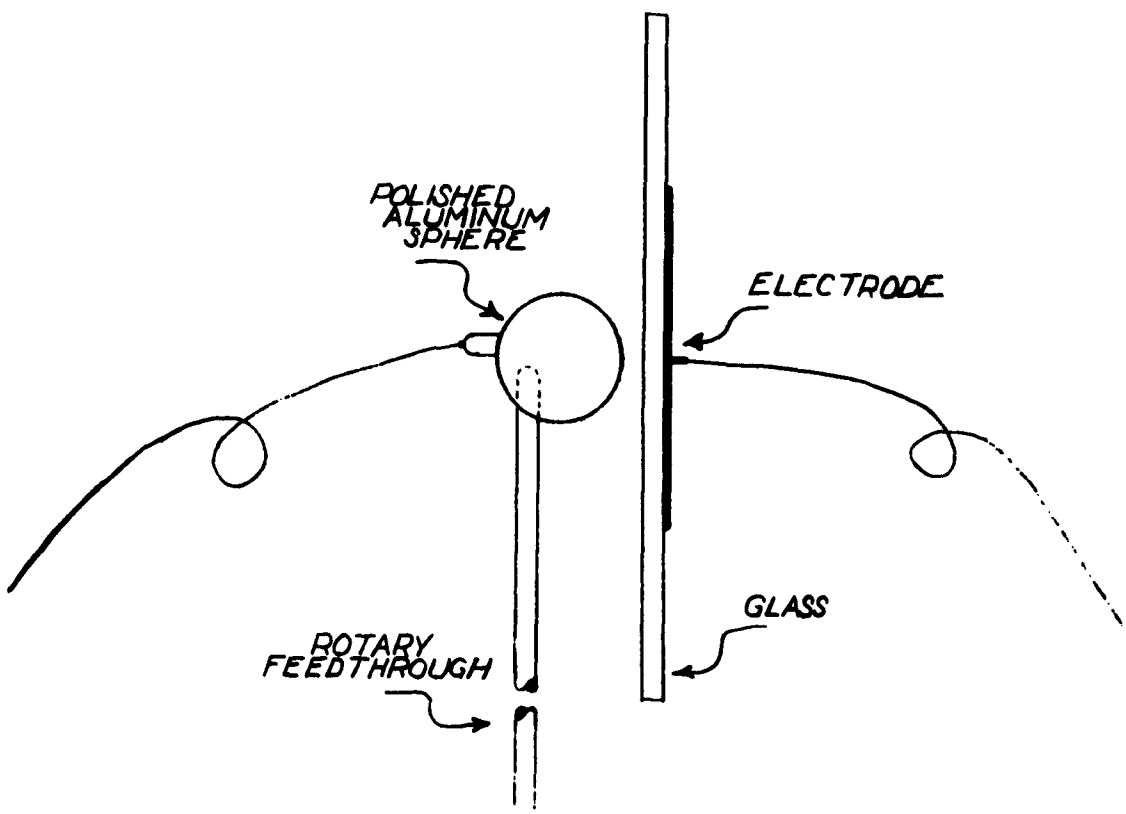

Figure 16. Typical Setup for the Vacuum Breakdown Tests

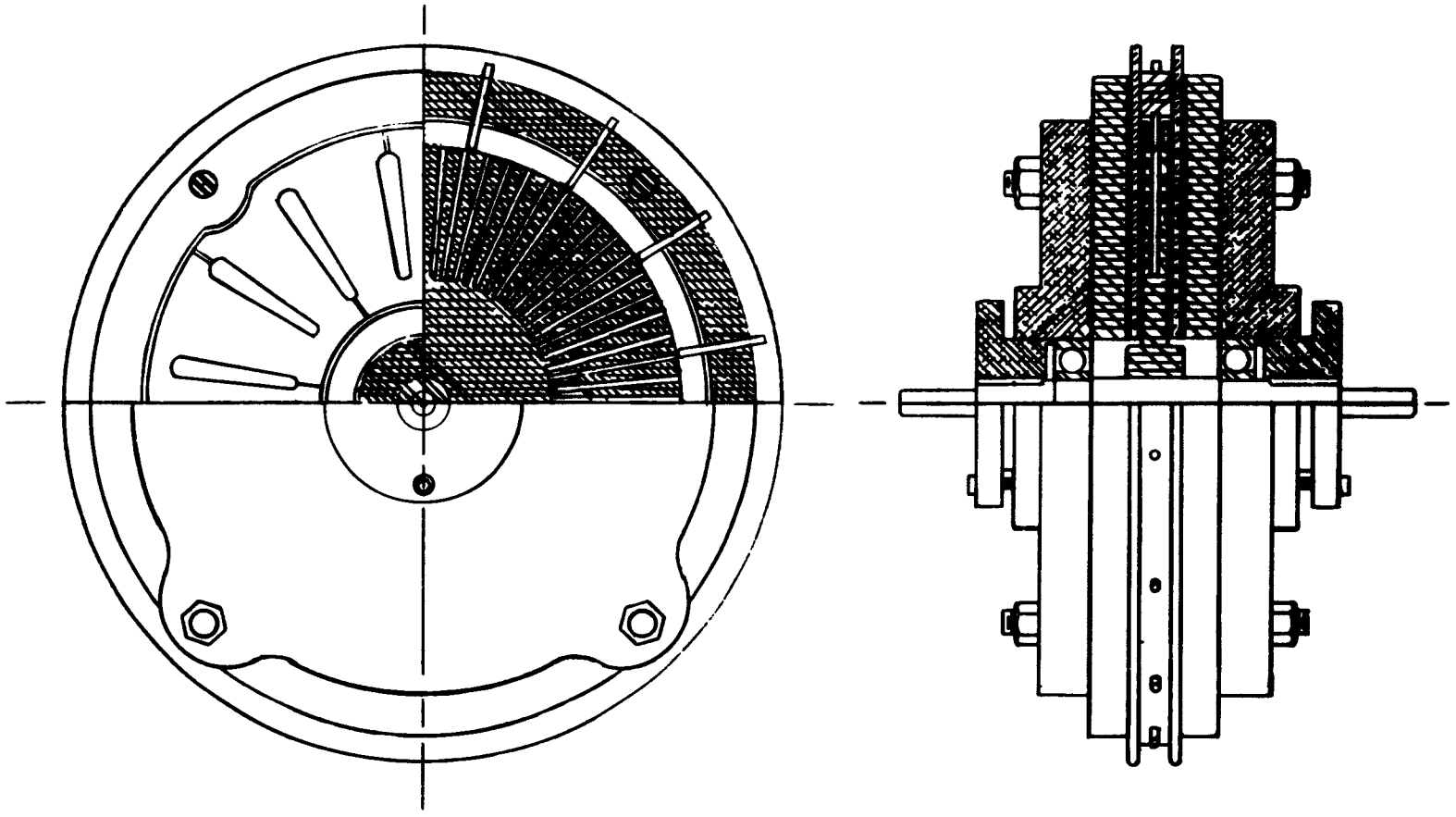

Figure 17. Vacuum-Insulated Constant Oblique Field Electrostatic Generator

are the same as those of the air model----5-inch effective diameter, 5½-inch over-all diameter, commutator groove ¼ of an inch deep, rotor thickness ½ of an inch, and 72 charge carriers 1¼ of an inch long.

Seventy-two charge carriers were made by metallising holes drilled in the rotor. First, however, short (1/8-inch) hollow brass inserts were screwed in the ends of the holes to act as a wearing surface for the commutator. Before metallising the holes, the rotor was tested, using only these inserts as charge carriers.

A test stator was fabricated for preliminary testing. This stator had three pairs of poles, one pair spaced to correspond to a four, one pair to an eight, and one pair to a sixteen-pole machine. In anticipation of a substantial increase in output voltage for vacuum operation, a sixteen-pole machine was envisioned. The test stator would check the validity of this assumption. The stator was made by painting narrow 5-degree inductors on the glass, semi-conducting dielectric plate and bonding this plate to a Mycalex or glass-backing disk with an epoxy resin. With this construction the only organic material exposed to the high vacuum environment was the narrow band of epoxy at the edge and at the center hole of the disk. The inductor leads were brought out through the back of the stator. In anticipation of the results of this test, eight and sixteen-pole stators were fabricated.

Gap-type brushes were built that could be adjusted with less than one one-thousandths of an inch clearance between the end of the brush and the end of the charge carriers. The brushes were machined to a sharp point to promote discharges. Molybdenum disulfide lubricated bearings were used.

The generator was mounted on the base plate of the oil diffusion pump high vacuum unit. The unit was enclosed with an 18-inch diameter, 30-inch high glass bell jar. Located in the base plate were a 150 KV and a 50 KV feedthrough, in addition to several low voltage feedthroughs. A rotary magnetic feedthrough was provided to drive the generator from outside the vacuum chamber. The diffusion pump has a chevron-type, water-cooled baffle to inhibit migration of any oil into the high vacuum chamber. In addition, a liquid nitrogen cold trap is located just above the baffle in the high vacuum manifold.

Fig. 18 shows the three rotors. The 72-charge carrier, epoxy rotor is on the left; the glass-bonded mica rotor is in the center and the 144-charge carrier, epoxy rotor is on the right. Fig. 19 shows one of the brush holders, the glass-bonded mica rotor and one sixteen-pole stator. Fig. 20 shows three glass-bonded mica-backed stators in the foreground. The rotor is mounted on the test stand behind the stators. Fig. 21 shows the generator mounted on the vacuum chamber baseplate. The 150 KV bushing is in the background, and the 50 KV bushing is on the right. One of the glass-backed test stators is seen. This stator is designed to test two poles of a sixteen-pole generator.

3.3.2 Tests----Vacuum-Insulated Model

All vacuum tests were conducted in a pressure between 8×10^{-7} and 2×10^{-7} mmHg. The pressure was measured with a hot-cathode ionization gauge located in the high vacuum manifold. In the beginning, when a component was installed in the vacuum chamber for the first time, a pump-down of at least 24 hours was made before conducting any tests. Later, it was found that if these components were placed in the chamber at the top of the bell jar, they did not interfere with the tests and a great deal of time was saved between tests for the components were continuously being "vacuum conditioned". All components were thoroughly washed with a suitable solvent, followed by acetone, prior to installation.

The plan was to first test the generator at 1,775 rpm with only the 1/8-inch hollow inserts as charge carriers and with one stator instead of the usual two to facilitate changes. The first stator to be used was the test stator with the three specially-spaced pairs of inductors. The results of these tests would determine the influence of the distance between the poles.

Static tests were conducted on the stator. In air, better than 30 KV was applied to the inductors and no excitation current could be observed. In vacuum, however, discharges occurred in and around the glass tubing used to bring the inductor connections out of the stator. These discharges were reduced by removing as much of the tubing as possible. Apparently, the tubing trapped gases, which ionized upon being subjected to an electric field.

Figure 18. View of Three Generator Rotors

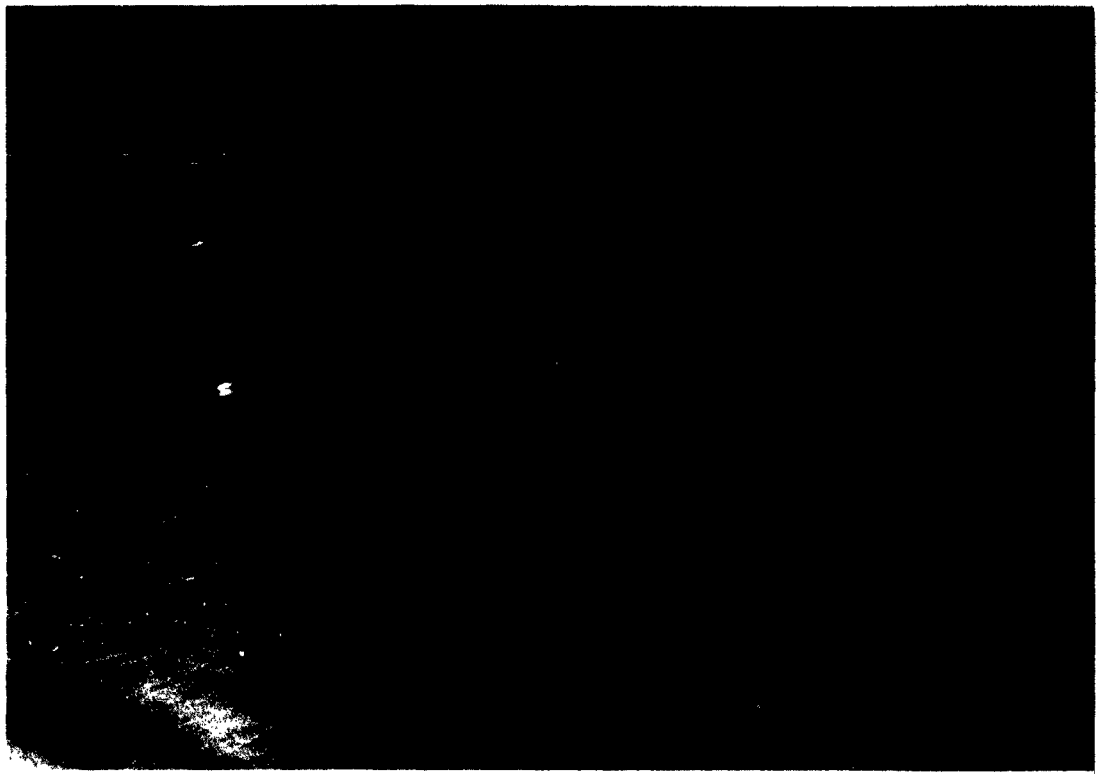

Figure 19. View of the Brush Ring, Rotor and Stator of the Vacuum-Insulated Generator

Figure 20. View of Three Test Stators and One Rotor for the Vacuum-Insulated Generator

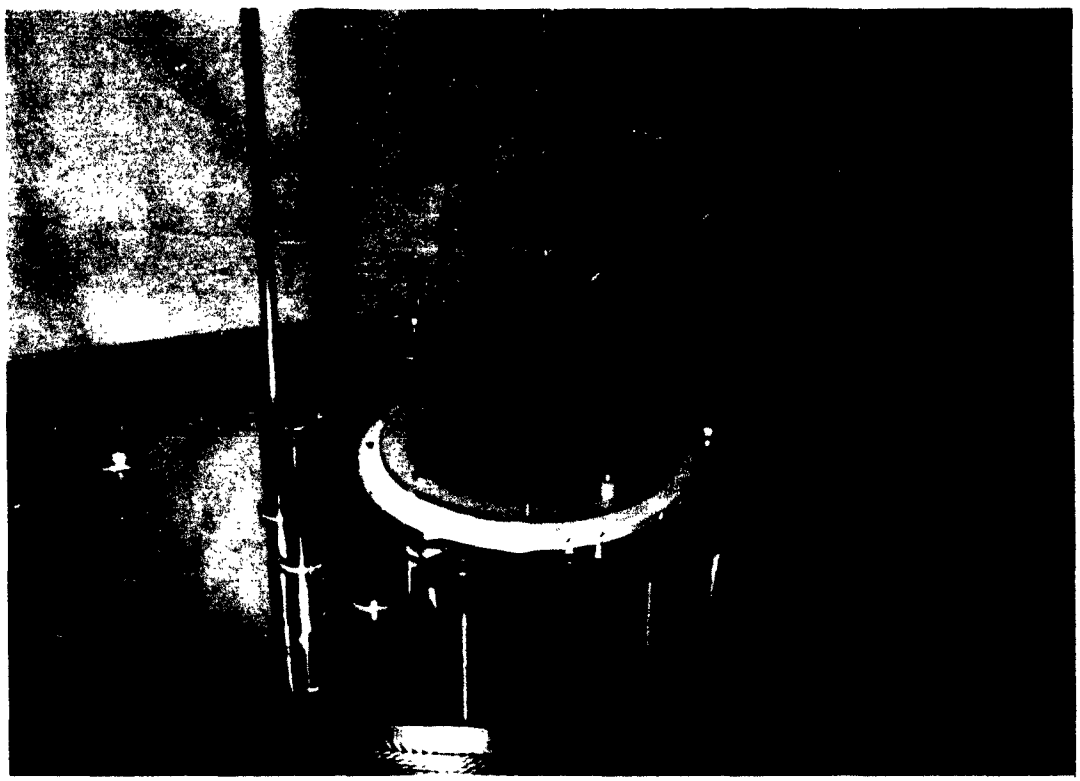

Figure 21. View of the Vacuum-Insulated Generator Mounted on the Vacuum Chamber Baseplate

The generator was first tested in air and operated perfectly. In vacuum, however, there was no output. A two-pole stator and gap-type brushes were being used. The brushes were then adjusted so close to the commutator that they actually touched at several points. Now, some current, one or two micro-amps, was generated in short circuit. The charge-carrier holes in the rotor were plated. The short-circuit current now was 2 or 3 micro-amps.

The non-contact type of brush was discarded. Contact-type brushes were then fabricated. The following types were fabricated and tested:

a) single wire
b) flexible strip
c) ball
d) multiple wire
e) silver graphite
f) oilite

Little success was experienced with the strip-type of brush but sufficient output was generated with each of the other five brushes to plot a curve (Fig. 22) of output current vs. output voltage. All five brushes produced about the same results. Additional tests indicated that poor commutation apparently was responsible for the low output obtained.

The 144-charge carrier, epoxy rotor was re-designed. The commutator shield was machined off and the epoxy removed from around the tips of the charge carriers. Then the ends of the charge carriers were carefully machined so that the surface was smooth and concentric. Now the brushes contacted only the charge carriers and they were designed to bridge three charge carriers to reduce brush bounce to a minimum. The two brush materials that seemed to perform best in the previous tests, silver graphite and oilite, were used with the new commutator. A substantial improvement in output was now obtained. Fig. 23 shows the short-circuit output current as a function of excitation voltage for a two-pole stator with sixteen-pole generator spacing. Fig. 24 shows the output current as a function of output voltage for three excitation voltages. The 34 KV excitation power curve, Fig. 24, has been extrapolated from the excitation curve of Fig. 23. The

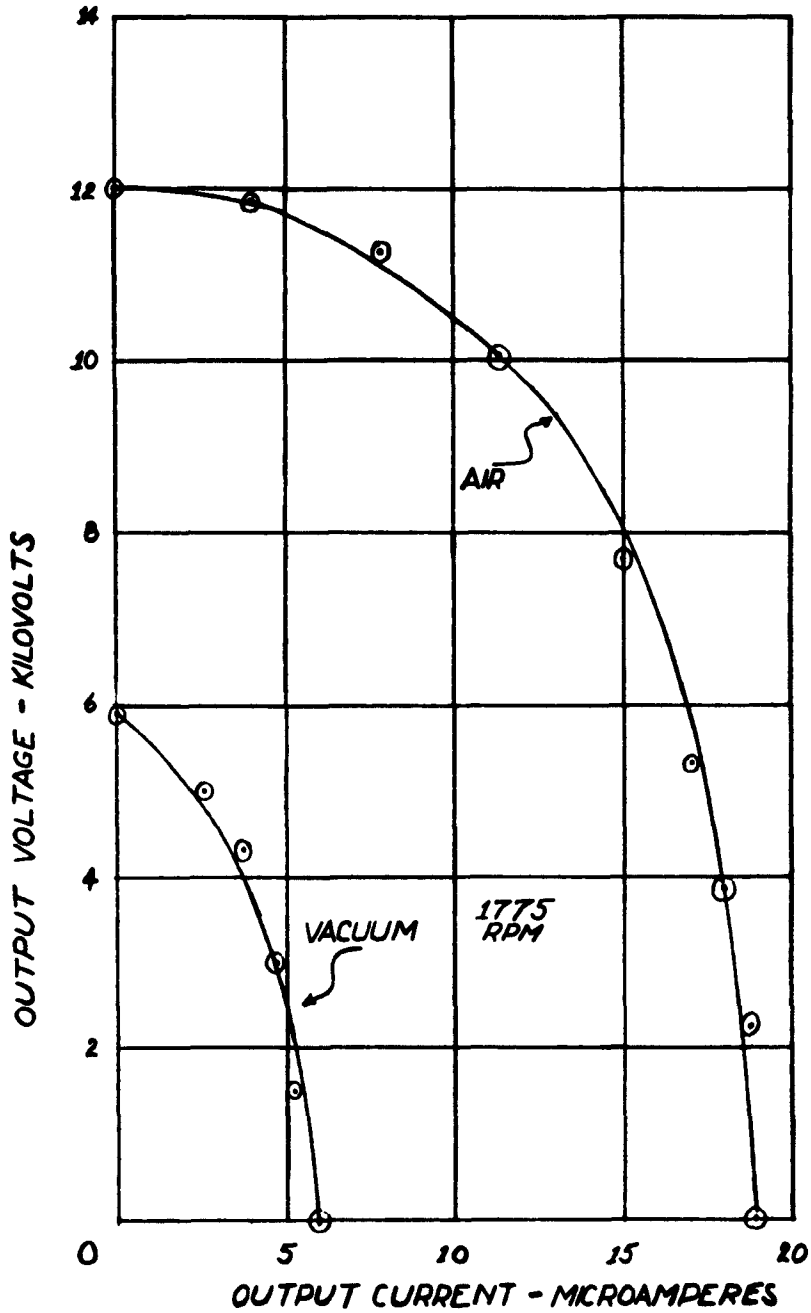

Figure 22. Output Voltage vs Output Current for the Vacuum-Insulated Generator

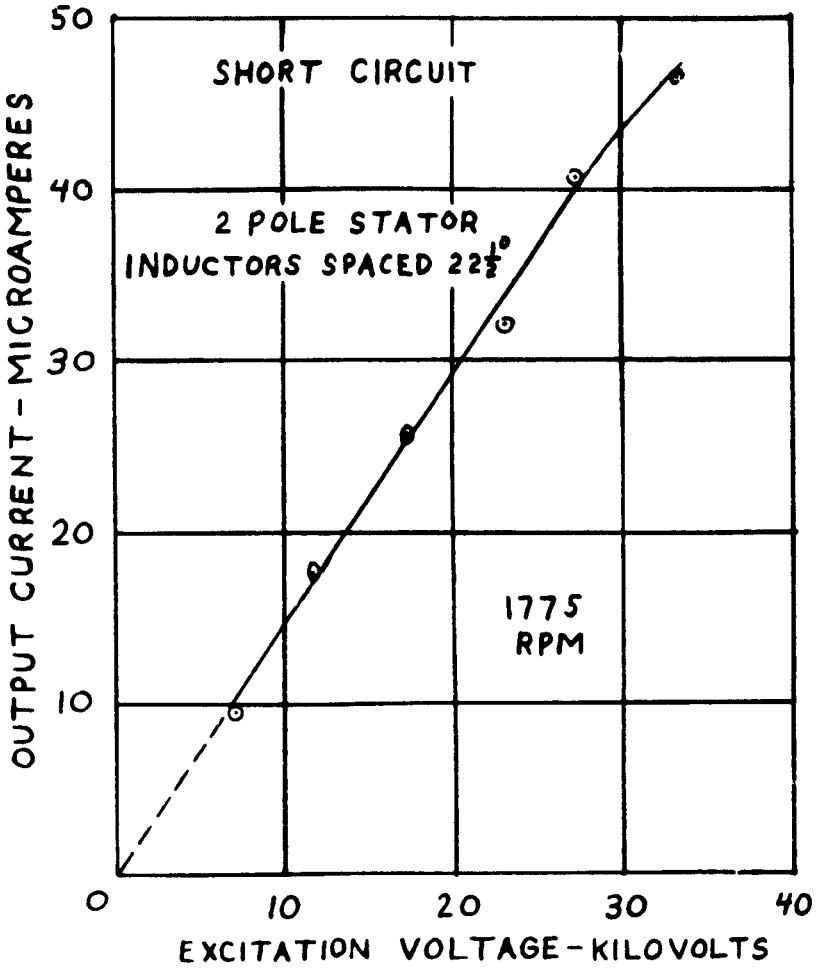

Figure 23. Output Current vs Excitation Voltage for the Vacuum-Insulated Generator

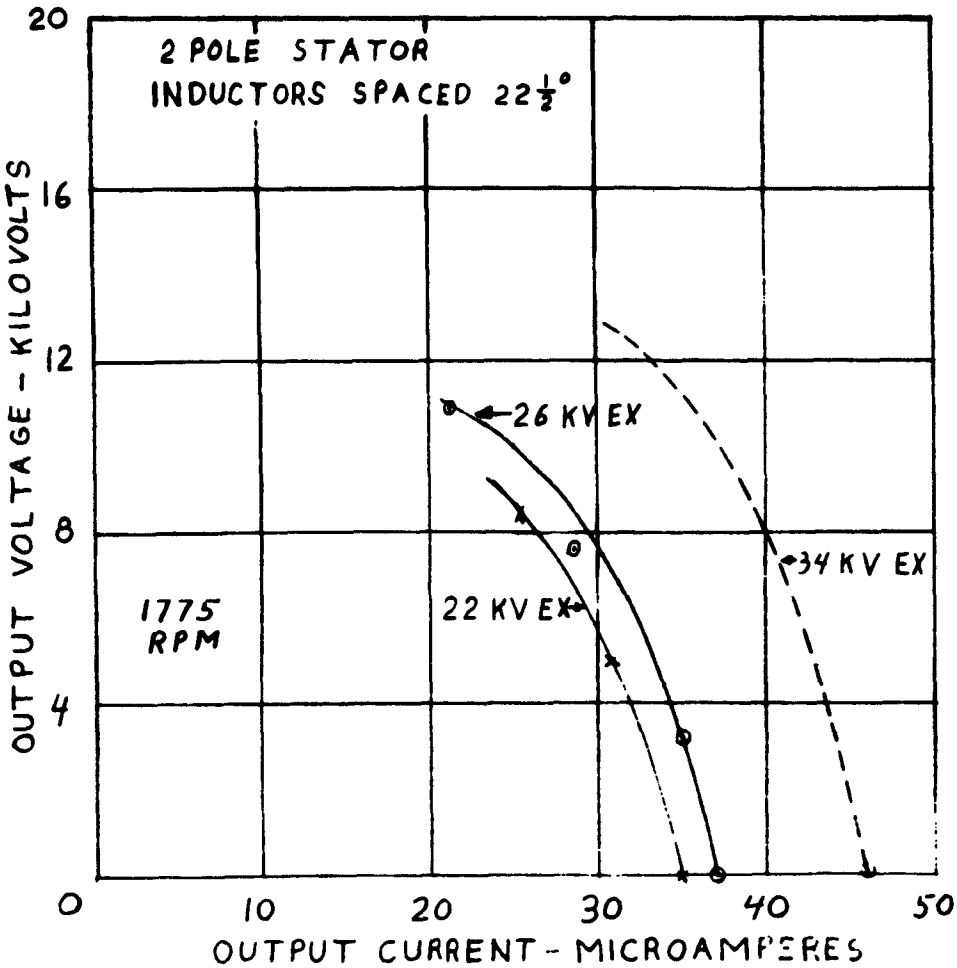

Figure 24. Output Voltage vs Output Current for the Vacuum-Insulated Generator

highest excitation voltage that could be attained without breakdown was 36 KV but no value for output could be obtained at this point. Breakdown occurred outside the rotor-stator gap. Improvement in geometry of the generator would be required to obtain higher excitation values. Fig. 23 indicates that the maximum field strength permitted in the gap has not been reached. With 27 KV excitation, the normalized power is 27 newtons/meter^2 and with the extrapolated 34 KV excitation power curve, the normalized power is 53 newtons/meter^2.

It was not possible to obtain sufficient data to calculate the efficiency of the vacuum-insulated generator. The generator output was drowned by the drive requirements.

Fig. 25 shows the instrumentation setup for the tests.

3.4 Summary

The advantage to be gained by use of a semi-conducting dielectric stator in a constant oblique field electrostatic generator has been demonstrated in the air tests. The power realized by use of such a stator was better than twice that of a generator with exposed inductors for the same excitation voltage and better than five times when the excitation voltage was raised to the optimal value permitted by the semi-conducting dielectric.

The results obtained in air yield a power of 12.5 watts at 15,000 rpm. The normalized power is 20 newtons/meter^2 which compares favorably with vacuum-insulated generators reported to date.

The technical literature shows that the dielectric strength of vacuum is about ten times that of air. This result has been verified by Cosmic, Inc. and gradients of 30 KV/mm have been obtained. From these considerations, it appears that an increase of power by a factor of 50 or 100 should be expected when replacing air by vacuum as a dielectric. In tests accomplished by Cleveland Pneumatic Industries, the power of the same machine was 80 milliwatts in air and 1.6 watts in vacuum, i.e., an increase by a factor of about 20, despite the fact that the machine contained a large amount of organic material. Consequently,

Figure 25. Instrumentation Setup for the Vacuum Generator Tests (From Left) Corona Load, Output Current, Output Voltage, Excitation Voltage, Excitation Voltage Power Supply, Vacuum Gauge Control (Below Table) Excitation Leakage Current, Input Brush Current, Vacuum Unit

the machine built at Cosmic, Inc. under the present contract should be capable of a power of 250 watts to 1.2 kilowatts, i.e., a normalized power of 400 to 2,000 newtons/meter^2. However, the tests accomplished have resulted in a power of 16.7 watts at 15,000 rpm, i.e., a normalized power of 27 newtons/meter^2. Fig. 26 is a comparison of the normalized power of three generators. It illustrates the fact that there is still much improvement to be expected in the performance of the vacuum-insulated c.o.f. generator.

3.5 Extrapolation to High Speeds

The constant oblique field generator is well-suited for operation at very high speed. The problem has been examined both from the standpoint of mechanical stress analysis and from the standpoint of vibration. Calculations of the power produced by a given machine may be immediately determined from the normalized power.

Actual power = normalized power $\times \frac{7R^3n}{36}$. An average fiberglass-reinforced epoxy resin may have a maximum allowable stress of 40,000 psi. For this material and a rotor having a thickness at the hub equal to twice the thickness of the charge carrier section with the two areas connected by a hyperbolic section, rotation at 24,000 rpm is possible with a rotor radius of 8 inches or 0.2 meters.

For such a generator the actual power is equal to the normalized power x 37. For instance, with a normalized power of 20 newtons/meter^2 the output would be 740 watts in air and with a normalized power of 400 to be expected in vacuum, the power would be 15 kilowatts. No inorganic material has been found in this program which would sustain as high a stress as a fiberglass-reinforced epoxy but it is expected that such a material could be developed.

The shaft of the generator will be subject to the same vibrations as any other high-speed, rotating device. One potential source of vibration peculiar to this type of generator has been analyzed here. The retarding force applied to each charge carrier is interrupted very briefly while the carrier is adjacent

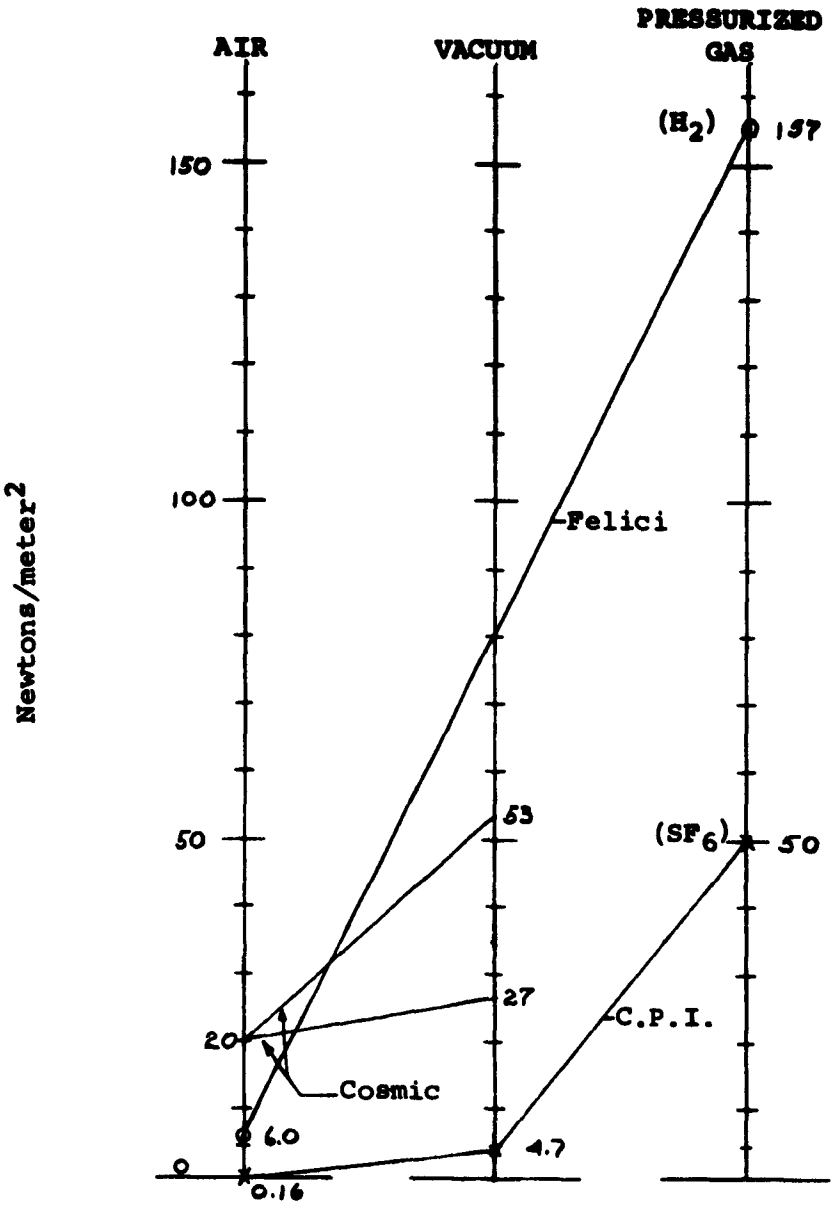

Figure 26. Comparison of Normalized Power of the Following Generators

Cosmic: Constant-oblique field generator
C.P.I.: Single capacitor--three elements machine tested by Cleveland Pneumatic Industries
Felici: Commercial insulating carrier generator

to an inductor. For a 144-charge carrier rotor at 24,000 rpm, variations of the torque are transmitted to the rotor at a frequency of 5.76 kilocycles which in turn has to be multiplied by the number of rotors mounted on the same shaft. A significant natural frequency of vibration for a rotor would not likely exist at this frequency.

4. Conclusions and Recommendations

The air tests have proved the feasiblility of the constant oblique field generator and have demonstrated this model as capable of higher power-to-weight ratios than other known types of generators. The vacuum tests have yielded an output higher than that obtained in air but still an order of magnitude lower than that which can be predicted from the experimental data on vacuum breakdown.

It is recommended that further studies be undertaken on this concept of generator and that they include:

1) Experimentation of various commutation methods;
2) Construction of a one-disk generator capable of rotating at high speed;
3) Construction of a compact assembly of several rotors on the same shaft.

REFERENCES

1. Dominique Gignoux, "Constant Oblique Field Electrostatic Generator", A.R.S. Space Power Systems Conference, Santa Monica, California, September 1962, preprint #2556-62.

2. N. J. Felici, Elektrostatische Hochspannungs-Generatoren, Verlag G. Braun, Karlsruhe, 1957.

3. A. A. Vorobyev, G. A. Vorobyev et al, Vysokoye Ispytatel'Noye Oborudovaniye I Izmereniya, State Publishing House of Energetics, Moscow - Leningrad, 1960.

4. Roger Morel, Contribution à l'Étude Rationnelle des Machines Électrostatiques, edité par Les Annales de l'Université de Grenoble, Institut Fourier, Grenoble, 1948.

5. Élie Gartner and Noel J. Felici, Contribution à l'Étude des Génératrices Électrostatiques à Transporteurs Isolants; RGE, 12, Place Henri-Bergson, 12, Paris (VIII^{e}), 1953.

6. E. Durand, Électrostatique et Magnétostatique, Masson & Cie, Paris (VI^{e}), 1953.

7. R. Hawley and A. Maitland, "Vacuum as an Electric Insulator: A Bibliography", C. A. Parsons and Co., Ltd., Newcastle upon Tyne, 6, England.

8. Joseph J. Murray, "Glass Cathodes in Vacuum-Insulated High-Voltage Systems", Lawrence Radiation Laboratory, Berkeley, California.

9. Ion Physics Corporation, Quarterly Technical Progress Report No. 1, AF 33(616)-7230, Burlington, Massachusetts, 22 August 1962.

Aeronautical Systems Division, Dir/ Aeromechanics, Flight Accessories Lab, Wright-Patterson AFB, Ohio.
Rpt No. ASD-TDR-63-87. CONSTANT OBLIQUE FIELD, ELECTROSTATIC GENERATION. Final report, Apr 63 53pp. incl illus., 9 refs.
Unclassified Report

The principle of operation of the constant oblique field, electrostatic generator is described and the increase in power obtained from a generator featuring this field arrangement is predicted from theoretical investigations. A generator has been built and tested in air and in vacuum environment of 2 x 10^{-7} to 7 x 10^{-7} mm Hg. The results

(over)

of the tests in air have met those anticipated. A five-inch diameter rotor has produced a power of 12.5 watts at 15,000rpm. The vacuum tests have yielded values somewhat greater than those obtained in air, whereas data from previous experimenters show that an increase in power by a factor of 50-100 should be expected.

1. Electrostatic generator
I. AFSC Project 8128, Task 812808
II. Contract No. AF 33(657)-7769
III. Cosmic, Inc., Washington, D. C.
IV. Hermann Anton, Dominique Gignoux John J. Shea
V. Secondary Rpt No. 41
VI. Not aval fr OTS
VII. In ASTIA collection

Aeronautical Systems Division, Dir/ Aeromechanics, Flight Accessories Lab, Wright-Patterson AFB, Ohio.
Rpt No. ASD-TDR-63-87. CONSTANT OBLIQUE FIELD, ELECTROSTATIC GENERATION. Final report, Apr 63 53pp. incl illus., 9 refs.
Unclassified Report

The principle of operation of the constant oblique field, electrostatic generator is described and the increase in power obtained from a generator featuring this field arrangement is predicted from theoretical investigations. A generator has been built and tested in air and in vacuum environment of 2 x 10^{-7} to 7 x 10^{-7} mm Hg. The results

(over)

of the tests in air have met those anticipated. A five-inch diameter rotor has produced a power of 12.5 watts at 15,000rpm. The vacuum tests have yielded values somewhat greater than those obtained in air, whereas data from previous experimenters show that an increase in power by a factor of 50-100 should be expected.

1. Electrostatic generator
I. AFSC Project 8128, Task 812808
II. Contract No. AF 33(657)-7769
III. Cosmic, Inc., Washington, D. C.
IV. Hermann Anton, Dominique Gignoux John J. Shea
V. Secondary Rpt No. 41
VI. Not aval fr OTS
VII. In ASTIA collection